

# Covalently Crosslinked Mussel Byssus Protein-Based Materials with Tunable Properties

*<sup>1,2</sup>Frédéric Byette, <sup>2</sup>Isabelle Marcotte\*, <sup>1</sup>Christian Pellerin\**

<sup>1</sup>Département de chimie, Université de Montréal, Montréal, Québec, H3C 3J7, Canada

<sup>2</sup>Département de chimie, Université du Québec à Montréal, Montréal, Québec, H3C 3P8,  
Canada

## Corresponding authors:

\*Isabelle Marcotte:

Phone: +1 514 987 3000 ext. 5015; Fax: +1 514 987 4054

E-mail: [marcotte.isabelle@uqam.ca](mailto:marcotte.isabelle@uqam.ca)

\*Christian Pellerin:

Phone: +1 514 340 5762; Fax: +1 514 340 5290

E-mail: [c.pellerin@umontreal.ca](mailto:c.pellerin@umontreal.ca)

## Keywords :

Peptide-based material, Mechanical properties, Protein crosslinking, Infrared spectroscopy, Biopolymer

## **Abstract**

Mussels' anchoring threads, named byssus, are collagen-rich fibers with outstanding mechanical properties. Our previous work has shown the possibility to produce a byssus protein hydrolyzate with good film-forming ability, providing a promising new avenue for the preparation of biomaterials. Materials prepared from regenerated fibrous proteins often need additional treatments to reach the performance required for targeted applications. Here, we studied the effect of covalent crosslinking, using a carbodiimide or glutaraldehyde, on the mechanical properties and enzymatic resistance of byssus-based materials. The results show that the mechanical properties of the films can be tuned, and that a higher crosslinking degree leads to increases in modulus and strength accompanied by a loss of extensibility. Structural analysis performed by infrared spectroscopy revealed that crosslinking induces an unexpected transition from aggregated strands to hydrated collagen/PPII-related helical structures. The materials were nevertheless more resistant to collagenase degradation as a result of higher crosslinking density. This new set of materials prepared in aqueous environment could find a niche in tissue engineering.

## 1 Introduction

The byssus is a complex fibrous protein-based set of anchoring threads whose role is to secure mussels from water perturbations such as currents, waves and tides. Studies carried out on Mytilid species have shown that the entire byssus fiber is covered with a thin cuticle ending with a plaque, both made from the same family of mussel foot proteins (mfp's).<sup>1</sup> The mfp's contain a large amount of dihydroxyphenylalanine (DOPA) that can form complexes with metals and contribute to the strength and extensibility of the cuticle and to the strong adhesion of the plaque to water-immersed solid substrates.<sup>1-6</sup> The core of each byssal thread is composed of three block copolymer-like proteins having a central collagenous domain flanked by either silk, elastin or glycine rich domains and histidine-rich termini on both sides.<sup>7</sup> The graded distribution and particular head-to-head/tail-to-tail assembly of these block copolymers in the byssus lead to the formation of oriented fibrils that provide strength and extensibility to the fibers.<sup>8,9</sup> The proteins in the native byssus are highly crosslinked by either covalent di-DOPA bridges, disulfide bridges, or organometallic coordination compounds.<sup>10</sup> An additional important aspect of the byssus fiber is the self-healing ability of its mechanical properties.<sup>11</sup> This behavior was ascribed to histidine/metal coordination compounds that can collapse under deformation and reassemble under rest, as well as to protein domains that can unfold reversibly.<sup>12,13</sup>

In our previous study using the byssus of the blue mussel *Mytilus edulis*, we showed the possibility of producing a byssus protein hydrolyzate (BPH) that can form films with pH-tunable mechanical properties.<sup>14</sup> This was attributed to the presence of charged amino acids, such as aspartic and glutamic acids, lysine, and arginine, which account for ~30 mol % of the total amino acid content. These residues offer the additional advantage of being

easily accessible for a wide range of chemical modifications. We also showed that films with self-healing capability and tunable mechanical properties can be prepared from BPH by exploiting the crosslinking with multivalent ions such as  $\text{Ca}^{+2}$  and  $\text{Fe}^{+3}$ .<sup>15</sup>

Fibrous protein-based materials are good candidates for soft tissue engineering since they offer potential biocompatibility, biodegradability, and low immunogenicity due to their biochemical nature similar (or identical) to macromolecules the human biological environment can recognize and metabolize. Indeed, silk, collagen and elastin have all been successfully applied for the production of biomaterials.<sup>16-21</sup> The repetitive primary amino acid sequence of fibrous proteins often drives the self-assembly of stable secondary structures that result in the formation of fibrous materials with impressive mechanical properties.<sup>16,22</sup> Many studies have highlighted the possibility of generating anisotropic structures by exploiting the hierarchical self-assembly of proteins and peptides with repeated motifs.<sup>23-27</sup> While regenerated fibrous proteins usually lead to self-standing materials that can be formed into a desired shape (such as films or 3D porous scaffolds); however, their mechanical properties and stability in a biological environment must often be tuned or improved in order to fulfill the application requirements.<sup>28-31</sup> Chemical reagents like carbodiimides or glutaraldehyde are often used to covalently crosslink proteins, through reactions with the carboxylic acid and amino groups of the side chains and termini. Although glutaraldehyde is known for its adverse effect on the biocompatibility of biomaterials as it is cytotoxic and induces acute inflammatory response from the host,<sup>32</sup> EDC reaction leads to water soluble molecules that can be easily removed following washing steps, which helps to preserve the biocompatibility of the materials.<sup>33</sup> Such

crosslinking methods have been successfully applied to adjust the mechanical properties and/or biological response of biomaterials made of collagen and elastin.<sup>34-39</sup>

The objective of this work was thus to enhance the mechanical strength and the resistance to enzymatic degradation of mussel byssus-derived BPH films by using chemical crosslinking with carbodiimide or glutaraldehyde. We show that chemically crosslinked BPH films are up to 10 times stiffer and 3 times stronger than the pristine films but that they partially lose their extensibility. Covalent crosslinking also renders the BPH films highly resistant to collagenase degradation. The capability of modulating the mechanical properties of the BPH-based materials is an asset for soft tissue engineering as it may enable matching the biomechanics of a wide range of biological tissues.

## **2 Material and Methods**

### **Materials**

Stocks of byssi were kindly provided by Moules de Culture des Îles Inc. (Magdalen Island, QC, Canada) and La Moule du Large (Magdalen Island, QC, Canada). Byssal threads were first sorted to remove most of the unwanted sea products (algae, shells and fish-related parts) then thoroughly washed with soap under tap water. The cleansed product was rinsed several times with distilled water and frozen at -20 °C. Except otherwise mentioned, all chemicals of reagent grade were purchased from Sigma-Aldrich (St-Louis, MO, USA) and used without further purification.

### **Methods**

*Byssal proteins hydrolyzate (BPH) preparation*

Extraction of proteins from the byssal threads was performed as previously reported.<sup>14</sup> Briefly, 5 g of cleansed and crushed dry byssus was magnetically stirred in 150 mL of extraction buffer containing 0.1 M sodium ethylene diamine tetraacetate (EDTA) adjusted to pH 13.5. After 7 days at 4 °C, the resulting slurry was centrifuged (Eppendorf centrifuge 5804R, Mississauga, ON, Canada) at 5000 rpm during 60 min at 4 °C to separate the solution from non-solubilized particles and the supernatant was filtered to remove any remaining foreign materials. Proteins in the supernatant were precipitated by adjusting the pH to 4.5 using acetic acid and by adding sodium chloride to reach a 0.5 M final concentration. The proteins were left to precipitate for 1h before being pelleted by centrifugation at 5000 rpm for 20 min at 4 °C. The precipitate was dispersed in distilled water before being dialyzed (SpectraPor 1, MWCO 6-8 kDa) (Spectrum Lab, Rancho Dominguez, CA, USA) for 3 days against distilled water. The precipitate was finally pelleted by centrifugation at 5000 rpm for 20 min at 4 °C before being freeze-dried.

### *Films preparation*

The foam-like lyophilized BPH was crushed and dispersed in water before adjusting the pH to 10.5 using sodium hydroxide (NaOH), reaching a final slurry concentration of 1 % (m/v). The solution was pulse sonicated for 1 min using a Microson XL 2000 ultrasonic homogenizer (Qsonica, Newtown, CT, USA). The solution was finally degassed by centrifugation for 2 min at 5000 rpm and 1 mL of the solution was poured into each well of a homemade Teflon mold (49 circular wells of 20 mm diameter). The solutions were left to evaporate under a fume hood until dry films were formed, usually for 96 h. The films were gently peeled off and washed with distilled water for 30 min before further treatments.

#### *EDC-NHS (EN) crosslinking of proteins in films*

BPH films were covalently crosslinked using 1-ethyl-3-(3-dimethylaminopropyl)carbodiimide (EDC) and *N*-hydroxysuccinimide (NHS). These films are labeled as EN throughout the study. The BPH films of about 10 mg dry weight were conditioned for 30 min in 5 mL of 50 mM 2-morpholinoethane sulphonic acid (MES) at pH 5.5. The films were subsequently crosslinked by immersion in 50 mM MES at pH 5.5 (4 mL/film) containing various concentration of EDC ranging from 0.1 to 10 mM and NHS, keeping the EDC:NHS molar ratio constant at 4:1. The reaction was left for 4 h then the films were washed once with 0.1 M Na<sub>2</sub>HPO<sub>4</sub> (pH 9.1) for 1 h to stop the reaction and rinsed with distilled water four times during 30 min.

#### *Glutaraldehyde crosslinking of proteins in films*

BPH films were chemically crosslinked by immersion in 5 mL glutaraldehyde (GTA) 2.5 vol% aqueous solution for 5 min at room temperature. Films were then rinsed with distilled water for 5 min to remove unreacted GTA, immersed in a 50 mM TRIS solution (pH 8.1) for 5 h to block any unreacted aldehyde groups, and finally rinsed with distilled water during four periods of 30 min.

#### *Blocked amino group content*

The free primary amino group content in films was determined spectrophotometrically after reaction with 2,4,6-trinitrobenzene sulphonic acid (TNBS) following the method of Bubnis *et al.* with slight modifications.<sup>40</sup> Film samples weighing

between 2 and 4 mg were incubated for 30 min in 0.5 mL of NaHCO<sub>3</sub> (4 wt %) solution. To this mixture, 0.5 mL of a freshly prepared TNBS solution (0.5 wt %) in NaHCO<sub>3</sub> (4 wt %) was added. After reaction for 2 h at 40 °C, 1.5 mL of 6 M HCl was added and the temperature was raised to 90 °C under magnetic stirring. Solubilization of films was achieved within 120 min. Then 2.5 mL of MilliQ water was added to the hydrolyzate and 10 mL of diethyl ether was used to remove excess TNBS and trinitrophenyl N-terminal amino acid. After three extractions, the aqueous layer was heated in a hot water bath (40 °C) for 15 min to evaporate residual ether and the absorbance was measured at 340 nm using a Biochrom Novaspec Plus (Cambridge, UK) spectrophotometer. A blank was prepared by the same procedure except that HCl was added prior to the addition of TNBS. The absorbance was correlated to the concentration of free amino groups, using a calibration curve generated with glycine, as:

$$[\text{NH}_2] = \frac{AV}{\epsilon l m_{\text{film}}} \quad (1)$$

where [NH<sub>2</sub>] is the free amino group content (mmol mg<sup>-1</sup>), *A* is the absorbance, *V* is the volume of the solution (mL), *ε* is the molar absorption coefficient of trinitrophenyl-glycine determined at 340 nm (13,000 mL mmol<sup>-1</sup> cm<sup>-1</sup>), *l* is the path length (cm) and *m<sub>film</sub>* is the dry weight of the sample (mg). The percentage of blocked amino group in crosslinked films was finally calculated, assuming 100% free amino groups in pristine films, according to the following equation:

$$\% \text{ blocked } \text{NH}_2 = \frac{[\text{NH}_2]_{\text{pristine}} - [\text{NH}_2]_{\text{crosslinked}}}{[\text{NH}_2]_{\text{pristine}}} \times 100 \quad (2)$$



### *Mechanical testing*

Single axial stress-strain measurements were conducted at 37 °C on sections (10 mm × 5 mm) of the various films using an Instron 5465 mechanical testing frame (Norwood, MA, USA) equipped with a 50 N load cell and a Biopuls bath filled with phosphate buffer saline (PBS) at pH 7.4. The films were mounted between the jaws and pre-conditioned in the PBS bath for ~2 min before applying a constant extension rate of 5 mm min<sup>-1</sup>. The modulus was calculated using the initial linear portion of the curve, typically between 2 and 5 % strain, and toughness determined from the area under the entire stress-strain curve.

### *Resistance to collagenase degradation*

The resistance of the BPH films to enzymatic degradation was assayed by exposing small pieces of materials to collagenase Type I from *Clostridium histolyticum* (125 U/mg). Pieces of films were first dried in an oven at 60 °C for 1 h and precisely weighed. Materials were then soaked for 1 h in TESCA buffer containing 50 mM TES, 2 mM CaCl<sub>2</sub> and 10 mM NaN<sub>3</sub> adjusted to pH 7.4. The films of ~3 mg were then transferred into 1 mL of collagenase solutions (1 mg/mL) prepared in the same buffer and incubated at 37 °C while agitating at 150 rpm in a Thermo Scientific MaxQ 4450 orbital shaker (Marietta, OH, USA). After 24 h, the samples were removed and soaked in 25 mM EDTA for 30 min at 60 °C to inactivate enzymes and remove calcium ions. Films were finally rinsed 3 times for 30 min with milliQ water and dried at 60 °C for 1 h before determining the remaining weight. A control was also performed by the same procedure in the absence of collagenase.

Pictures of the films were acquired using a Nikon Eclipse Ti inverted optical microscope (Mississauga, ON, Canada) equipped with a Nikon Digital Sight DS-Qi1Mc camera.

#### *Attenuated total reflection (ATR) Fourier transform infrared (FTIR) spectroscopy*

Infrared spectra of the films before (pristine) and after different treatments were obtained using a Bruker Optics Tensor 27 spectrometer (Billerica, MA, USA) with a liquid nitrogen-cooled mercury-cadmium-telluride detector and a Golden Gate diamond ATR accessory (Specac, Swedesboro, NJ, USA). Spectra of the films were acquired by averaging 256 scans at a  $4\text{ cm}^{-1}$  resolution. Each film was analyzed at three or four different locations and the resulting spectra were averaged to account for any possible inhomogeneity. Spectra were processed using LabSpec 6 spectroscopy suite v.6.2.69 (Horiba Scientific, Edison, NJ, USA) and GRAMS/AI v.7.00 (Thermo Fisher Scientific, Waltham, MA, USA). A linear baseline was applied in the amide A, I or II region of the spectra, i.e. between  $3700\text{-}2830\text{ cm}^{-1}$ ,  $1720\text{-}1580\text{ cm}^{-1}$  or  $1580\text{-}1480\text{ cm}^{-1}$  respectively, before normalizing using the area under the curves. Second derivative curves of the spectra were obtained using a Savitzky-Golay algorithm on 5-9 points before multiplying by -1 to invert the resulting traces. The traces were finally vector-normalized for easier comparison.

### **3 Results and discussion**

#### *Free amino groups and degree of crosslinking*

The BPH films are water insoluble as a result of the self-assembly of the polypeptides in stable molecular structures, i.e., intermolecular anti-parallel  $\beta$ -sheets and collagen triple helices.<sup>14</sup> The chemical crosslinking performed on the self-standing pristine

films was thus feasible in aqueous environment, which is an asset for peptide-based biomaterial development. The percentage of reacted (blocked) amino groups was first determined in order to evaluate the efficacy and extent of the chemical crosslinking. Fig. 1 shows that it increases from ~8 to ~35 % when the EN concentration used for the crosslinking reaction is raised from 0.1 to 5 mM and that it reaches a plateau for higher concentrations. The GTA crosslinking reaction led to ~38 % of blocked amino groups for the 5 min reaction time at the 2.5 % concentration used. In contrast with the carbodiimide reaction, it was possible to reach a much higher crosslinking density (up to ~80 % of blocked amino groups) when using higher GTA concentration and longer reaction time, i.e., 10 % for 24 h.

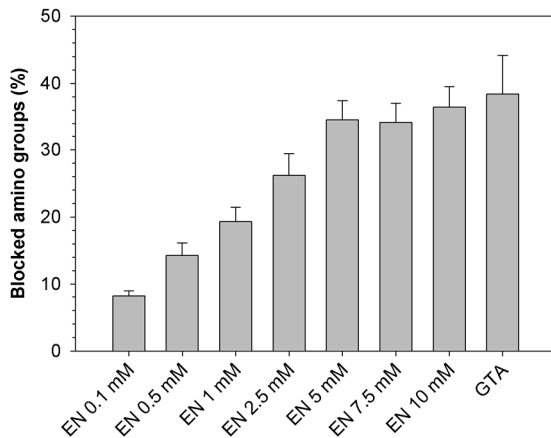


Fig. 1 Percentage of blocked amino groups in the EDC-NHS (EN) crosslinked and glutaraldehyde (GTA) crosslinked films relative to the pristine films as determined with the TNBS method. Results are the average value  $\pm$  standard deviation for N = 3.

The difference in the crosslinking density reached with EN and GTA treatment can be explained by their reaction mechanism. The EN reaction can take place in proteins only

between adjacent carboxylic acid and free amino groups to create a new amide bond. It is called a “zero-length” crosslinker because no additional segments are introduced during this reaction. The EN coupling is thus only possible within a distance of 1 nm so that sufficient mobility of the protein network is necessary for the reaction to occur.<sup>33,41</sup> On the other hand, GTA reacts with free amino groups, mainly from lysine’s side chains and N-termini of polypeptides chains, and incorporates a spacer of at least 5 carbons between crosslinked moieties. GTA is therefore a “long-range” crosslinking agent. Moreover, it can self-polymerize and react irreversibly with a single amino group, leaving a free aldehyde that must be quenched to stop its reactivity, for example with a small molecule having a reactive free amino group. Therefore, the lower percentage of amino groups blocked by the EN reaction may be attributed to the tight packing of the physically crosslinked secondary structure elements composing the BPH films, such as intra and intermolecular  $\beta$ -sheets. The limited molecular mobility of the amino and carboxylate groups buried within such protein domains would hinder the reaction and lead to the plateau seen in Fig. 1.

### ***Tensile mechanical properties***

The effect of covalent crosslinking on the mechanical performances of the various BPH films was assessed in a simulated biological environment (PBS-filled bath at 37 °C and pH 7.4) under tension mode. As reported in Fig. 2 and Table 1, both the modulus and the ultimate tensile strength (UTS) strongly increase, from 2 to 21 MPa and from 0.7 to 2.9 MPa, respectively, as the EN concentration increases from 0.1 to 10 mM. At the same time, the strain at fracture (SF), which was 0.6 for the pristine films, decreases from 0.4 to 0.23, thus resulting in a similar toughness ( $\sim 0.4 \text{ MJ m}^{-3}$ ) for all the EN crosslinked films. It is

well known that a higher crosslinking degree in hydrogels generally leads to increased stiffness and strength and a decrease in SF as it restricts the molecular motion of the network.<sup>42</sup> Our results suggest that the physical entanglements of the protein chains are trapped by the new covalent bonds introduced by crosslinking, thus leading to stiffer and stronger but less extensible materials with the increase in crosslinking density.

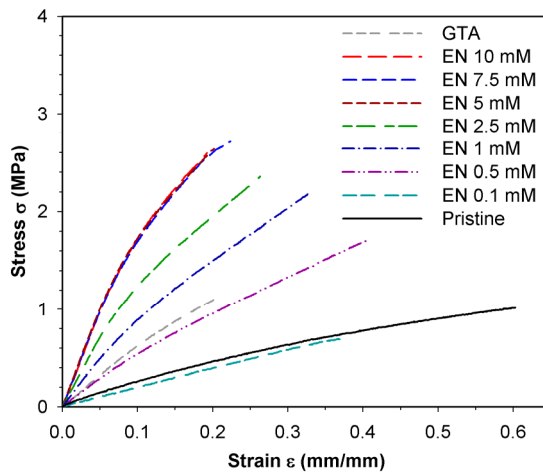


Fig. 2 Representative tensile stress-strain curves for the pristine BPH films and the EN and GTA crosslinked BPH films.

The mechanical properties of the crosslinked BPH films differ significantly from those of the distal part of *M. edulis* byssal threads, for which a modulus of 150 MPa and a strain at fracture of 0.9 mm/mm are reported.<sup>14</sup> This was expected since the production and purification process of the BPH do not allow conserving the structural integrity of the native proteins found in the byssal threads. Moreover, the level of hierarchical assembly of the proteins in the native threads could not be reproduced during the self-assembly of the BPH films. Finally, the proteins in the core of the byssus thread are highly oriented while they are isotropic in the matrix of the BPH films as observed using polarized optical

microscopy. Therefore, the mechanical performances of the BPH films are inferior to those of the native byssal threads, even following chemical crosslinking.

In good agreement with the crosslinking density results of Fig. 1, a plateau in the mechanical performance of the EN crosslinked materials can be observed above 5 mM. At this EN concentration, the side-chain mobility would become too low to form additional crosslinking points and the network probably confines most entanglements.

Table 1: Uniaxial tensile mechanical properties of the pristine BPH films and the EN and GTA crosslinked BPH films.

	Modulus (MPa)	UTS* (MPa)	SF* (mm/mm)	Toughness (MJ m <sup>-3</sup> )
Pristine	2.5 (0.2)	1.0 (0.2)	0.60 (0.03)	0.36 (0.08)
EN 0.1 mM	2.0 (0.2)	0.7 (0.1)	0.4 (0.1)	0.17 (0.05)
EN 0.5 mM	5.8 (0.7)	1.8 (0.4)	0.4 (0.1)	0.4 (0.2)
EN 1 mM	9.3 (0.9)	2.1 (0.4)	0.3 (0.1)	0.4 (0.2)
EN 2.5 mM	14 (2)	2.3 (0.3)	0.29 (0.06)	0.4 (0.1)
EN 5 mM	18 (2)	2.5 (0.7)	0.23 (0.08)	0.4 (0.2)
EN 7.5 mM	21 (2)	2.9 (0.3)	0.23 (0.05)	0.4 (0.1)
EN 10 mM	21 (2)	2.9 (0.5)	0.24 (0.06)	0.5 (0.2)
GTA	6.5 (0.5)	1.1 (0.3)	0.22 (0.06)	0.14 (0.08)

\*UTS: Ultimate tensile strength; SF: Strain at fracture. Average values (standard deviation),  $N \geq 6$ .

Fig. 2 and Table 1 show that, in contrast to the BPH films with a higher crosslinking density, the stiffness and UTS of the films crosslinked with the lowest EN concentration (0.1 mM) are slightly lower than those of the pristine films. In general, protein networks are physically stabilized by loci of adherence created by hydrogen bonds and hydrophobic

interactions from the backbone and side chains, which contribute to their mechanical properties. Crosslinking the proteins at the lowest EN concentration may create sufficient internal stress to disrupt some of these interactions without creating a sufficient density of covalent crosslinks to compensate for this effect, therefore leading to an initial loss of mechanical performance.

It can also be noted in Fig. 2 and Table 1 that films crosslinked with GTA were much weaker than those treated with EN at 5 to 10 mM, with a lower modulus by a factor 3, even though they had a very similar fraction of blocked amino groups (Fig. 1). The spacing introduced by the GTA long-range crosslinking seems to provide more flexibility to the network as compared to the EN coupling. In addition, the protein matrix of the GTA crosslinked films remains rich in free carboxylate groups at the experimental pH of 7.4, which leads to a higher water swelling of the hydrogel in PBS and to lower mechanical performance. Indeed, our previous work has shown that pristine films have pH-dependent mechanical properties: the electrostatic repulsion between charged amino acid side-chains in films treated at low or at high pH leads to more swelling and to lower strength and modulus than for films treated at their isoelectric point of 4.5. The higher mechanical properties obtained by EN crosslinking can also be explained by the nature of this coupling, i.e., between carboxylic acids and amino groups. Since the number of  $\epsilon$ -amino groups from lysine residues in the BPH is lower than the number of carboxylic acids from aspartic and glutamic acids (i.e. 5 vs 20 mol %),<sup>14</sup> EN can create twice the number of crosslinking points as compared to GTA. Interestingly, Fig. 2 and Table 1 show that the mechanical performances of the GTA crosslinked films fall between those of the films treated with EN at 0.5 and 1 mM, which have approximately half of the percentage of blocked amino groups

when compared to the GTA crosslinked films (Fig. 1). Thus, although electrostatic charges, type and size of crosslinker, chain entanglements, hydrogen bonding and hydrophobic interactions can all contribute to the mechanical performance of the GTA crosslinked films, the number of covalent crosslinking points seems to be the most important factor.

### ***Infrared spectroscopy analysis of the pristine and crosslinked BPH films***

FTIR spectroscopy was used to study the effect of chemical crosslinking on the molecular structure of the BPH films. The Amide A ( $\sim 3300\text{ cm}^{-1}$ ), Amide I ( $\sim 1630\text{ cm}^{-1}$ ) and Amide II ( $\sim 1515\text{ cm}^{-1}$ ) bands were analyzed and interpreted in terms of the two most abundant structures previously identified in BPH films, i.e., intermolecular anti-parallel  $\beta$  sheets (aggregated strands) and collagen/gelatin/polyproline II (PPII) helices. These structures have been identified in native byssal threads by infrared and NMR spectroscopy.<sup>43,44</sup> Intermolecular anti-parallel  $\beta$ -sheets, or aggregated strands, are composed of extended chains stabilized by strong hydrogen bonds between the carbonyl and amino groups of the polypeptide backbones, while collagen has a complex supercoiled structure made of three left-handed PPII helices.<sup>45</sup> The PPII helix is composed of a (Gly-X-Y)<sub>n</sub> repetitive motif where, in general, X and Y are proline and hydroxyproline residues, respectively. The PPII helices in native collagen are stabilized by intra- and intermolecular hydrogen bonds involving backbone carbonyls and water molecules. The following discussion will focus on the effect of EN crosslinking on the BPH films. Results for the GTA crosslinked films in the three Amide regions are shown in Fig. S1 of the Supporting Information.



Fig. 3a shows the spectra in the Amide I region of the pristine and EN-crosslinked films. This band originates from carbonyl stretching with minor contributions from in-plane N-H bending and C-N stretching within the protein backbone.<sup>45,46</sup> Its contour is greatly affected by the strength of hydrogen bonding and is therefore a good indicator of the protein secondary structure.<sup>45,46</sup> The first noticeable change in Fig. 3a is a gradual shift of the band maximum from 1627 to 1632  $\text{cm}^{-1}$  upon increasing the crosslinking degree. The maximal shift is reached at an EN concentration of 2.5 mM, as was observed for the mechanical properties (Fig. 2 and Table 1). In the second derivative spectra, a decrease of the 1620 and 1698  $\text{cm}^{-1}$  components, associated to intermolecular anti-parallel  $\beta$ -sheets (aggregated strands), is observed with increasing crosslinking density. This is accompanied by an increase of the components at 1660, 1644 and 1632  $\text{cm}^{-1}$  previously ascribed in the literature to collagen triple helix and/or to related model peptides with different structural folding or hydration state.<sup>47-50</sup> The simultaneous decrease of the 1620  $\text{cm}^{-1}$  component and increase of the 1632 and 1644  $\text{cm}^{-1}$  constituents result in the gradual blue shift of the Amide I band with increasing crosslinking. This is reinforced by the results from the Amide A and Amide II regions of the various BPH films (Fig. S2 and associated discussion in Supporting Information), where the formation of more hydrated structures was detected following the crosslinking reaction.

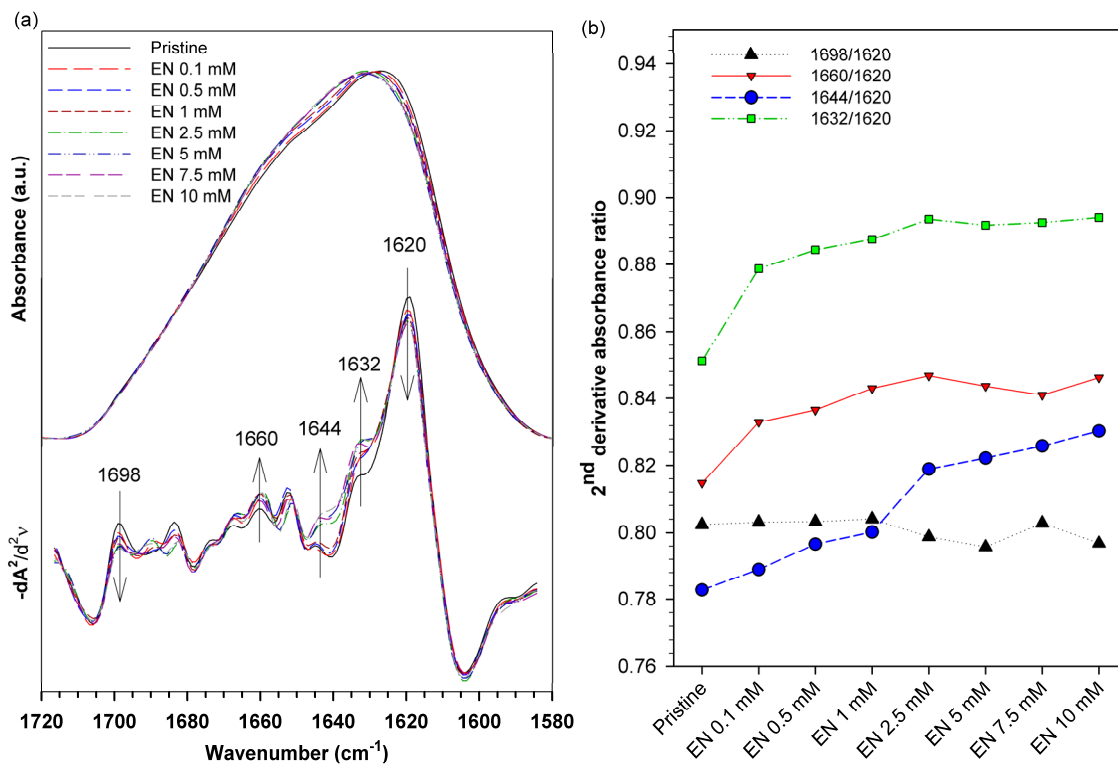


Fig. 3 (a) FTIR spectra in the Amide I region (top) and their corresponding second derivative (bottom) for pristine and crosslinked BPH films, and (b) intensity ratio of the second derivative components associated to aggregated strands (1620 and 1698 cm<sup>-1</sup>) and collagen-like structures (1660, 1644 and 1632 cm<sup>-1</sup>).

The evolution of the relative quantities of collagen-related structures and aggregated strands, as determined from the band components highlighted on the second derivative traces of Fig. 3a, is monitored as a function of EN concentration in Fig. 3b. The results are shown as intensity ratios with respect to the most intense component of the Amide I band at 1620 cm<sup>-1</sup>, which is due to aggregated strands, to help visualize the relative trends on a common scale. First, the 1698/1620 cm<sup>-1</sup> band ratio of the BPH films is unaffected by chemical crosslinking as expected since these two bands are both related to aggregated strands, which were shown to decrease during crosslinking. On the other hand,

the ratios for the 1660, 1644 and 1632 components increase with crosslinking density up to an EN concentration of 2.5 mM, followed by nearly constant values for higher EN concentrations. These results suggest that a partial structural conversion from aggregated strands to collagen/PPII related structures, albeit small (as seen from the absorbance and second derivative traces of Fig. 3a), occurs during the crosslinking process. The amplitude of this conversion increases with EN concentration until it plateaus at high crosslinking densities, in line with the observed mechanical performance in Fig. 2. Similarly to the films with low EN crosslinking degree, the spectra of the GTA-crosslinked films in the three Amide regions (Fig. S1) also point to a conversion from aggregated strands to hydrated collagen-related structures. In particular, the second derivative spectrum of GTA in the amide I region (Fig. S3) is similar to EN crosslinked films, with the same components ascribed to PPII/collagen structures, thus confirming that the changes detected are not occurring because of the formation of new amide bonds arising from the EDC reaction.

Hence, as depicted in Fig. 4, we propose that polypeptides in BPH films adopt more hydrated collagen or PPII-related structures following the covalent crosslinking reaction at the expense of the initially present aggregated strands. Although such disruption and structural conversion of aggregated strands could be *a priori* surprising considering their stabilization by strong hydrogen bonds, they can be partly explained by the release of a urea derivative during the crosslinking reaction with EDC-NHS. Urea is a well-known denaturing agent for proteins shown to induce the formation of PPII structures in short peptides and denatured proteins.<sup>51</sup> Treating hydrated pristine BPH films with urea at pH 4.5 led to FTIR spectra almost identical to those treated with 10 mM EN (Fig S4). Increasing the crosslinking density leads to higher urea derivative concentration during the

reaction and may disrupt some aggregated strands that would subsequently form hydrated PPII helices. These PPII helices could then lead to unordered collagen aggregates or coil which could then form collagen/gelatin triple helices, leading to the observed increase of the collagen and PPII-related bands and to the decrease of the anti-parallel  $\beta$ -sheet components in the infrared spectra.

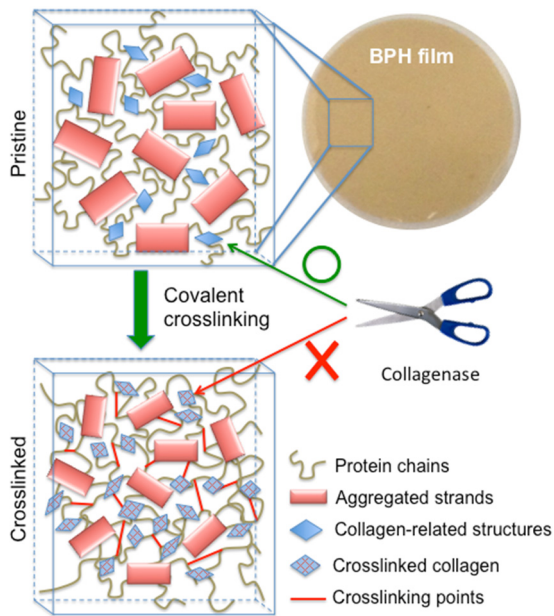


**Fig. 4** Representation of the protein network in the BPH films before and after the covalent crosslinking reaction. The aggregated strands (red) are partly converted into collagen-related structures (blue) and the crosslinked films become resistant to collagenase degradation.

#### ***Resistance to enzymatic degradation***

In view of possible application of the BPH materials and because our previous studies<sup>14,43</sup> have shown that both the byssus and its derived BPH films are rich in collagen, we evaluated the effect of covalent crosslinking on *in vitro* resistance toward collagenase

enzymatic degradation. A control made of type I collagen isolated from rat tail tendon was first incubated in the presence of the enzymes and was completely degraded after ~2 h. Pristine BPH films in the absence of collagenase were also used as a control and showed no weight loss. Fig. 5a shows that the pristine BPH films and 0.1 mM EN crosslinked films have a very similar susceptibility to collagenase degradation after 24 h of incubation, keeping about 70 % of their initial dry weight. This high resistance to enzymatic degradation could be explained by the fact that BPH is not exclusively composed of collagen but rather of a mixture of the many complex proteins forming the byssus threads, including aggregated strands as established by FTIR in the previous section. The resistance to enzymatic degradation is enhanced with the increase in chemical crosslinking density, as observed previously for dermal sheep collagen, collagen/hyaluronic acid scaffolds and ventral pericardium tissue.<sup>52-54</sup> A plateau where the collagenase has almost no degradation effect, i.e., with less than 5 % weight loss after 24 h, is reached at EN 2.5 mM, reminiscent of the plateau observed for the mechanical properties and for structural changes. Fig. 5a also reveals that collagenase degrades the GTA crosslinked films to an extent very similar to the 1 mM EN treated films, again bringing forward their similarity already noted in terms of degree of crosslinking and mechanical properties.

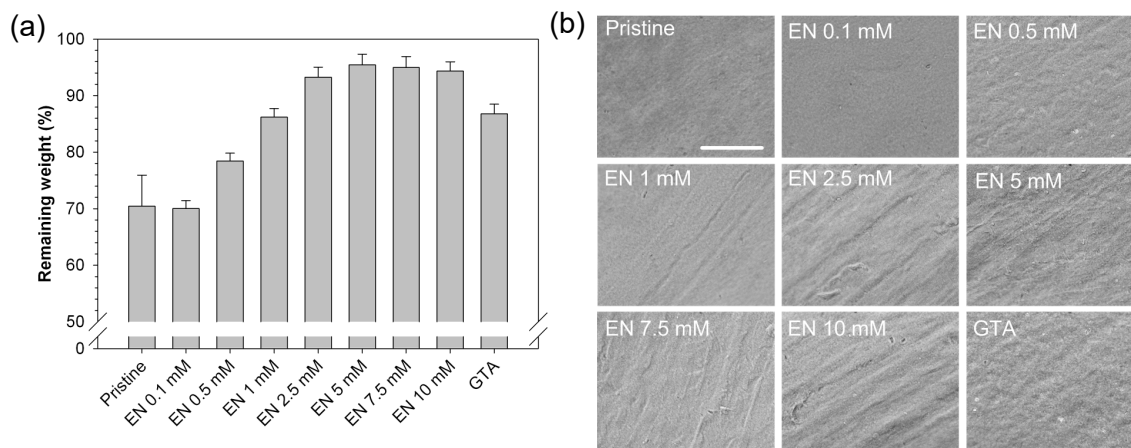


Fig. 5 (a) Resistance to collagenase degradation of the pristine, EN and GTA crosslinked BPH films after 24 h of incubation *in vitro*. Average  $\pm$  standard deviation,  $N \geq 3$ . (b) Optical microscopy images of the BPH films after incubation in the presence of collagenase. The scale bar is 100  $\mu\text{m}$ .

The optical microscopy results from Fig. 5b further demonstrate that pristine BPH films and those treated with low EN concentration and GTA are degraded by collagenase, as revealed by their smoother eroded surface following the incubation period. In contrast, films on which collagenase had almost no effect show a rougher surface where threads associated to the casting mold used to prepare the films can still be seen. Although EN treatment increases the proportion of collagen-related structural elements at the expense of aggregated strands (Fig. 3b), these collagen parts become less accessible to the enzyme due to the increased crosslinking in the films, as illustrated schematically in Fig. 4. The FTIR spectra of Fig. S5 confirm that the proportion of collagen-related components decreases compared to strands when exposing the pristine films to collagenase digestion. In contrast, the spectra of highly crosslinked BPH films are essentially the same before and after a 24 h enzymatic digestion, in line with the very small mass loss. These results highlight the excellent collagenase resistance of the BPH-based materials with high crosslinking density.

## **4 Conclusion**

In this study, we showed that chemical crosslinking using either glutaraldehyde or a carbodiimide (EDC-NHS) allows modulating the strength and stiffness of mussel-derived byssus protein hydrolyzate (BPH) films. As a result of increasing crosslinking density, the films become essentially resistant to collagenase degradation, which makes them potential candidates for biomaterials development. Using FTIR spectroscopy, we confirmed that the BPH films contain a relatively high amount of collagen as well as aggregated strands in anti-parallel  $\beta$  sheets conformation. An unexpected conversion of aggregated strands to collagen-related structure occurs when increasing the crosslinking degree. The ability to tune the mechanical properties of biomaterials is an asset for soft tissue engineering as it may extend their field of application and lead to a better biological response from the host. Thus, BPH films are a promising new set of protein-based biomaterials.

## **Acknowledgments**

This work was supported by a strategic research grant of the Natural Sciences and Engineering Research Council of Canada (NSERC) and funding from the Fonds de Recherche du Québec – Nature et Technologies (FRQNT). F.B. is grateful to the FRQNT and the Canadian Institutes of Health Research (CIHR) Strategic Training Initiative in Chemical Biology for the award of scholarships. I.M. is a member of Ressources Aquatiques Québec (RAQ) and C.P. is a member of the Centre Québécois sur les Matériaux Fonctionnels (CQMF).

## References

- [1] M. J. Harrington, A. Masic, N. Holten-Andersen, J. H. Waite, P. Fratzl, *Science* **2010**, 328, 216.
- [2] E. Degtyar, M. J. Harrington, Y. Politi, P. Fratzl, *Angew. Chem. Int. Ed.* **2014**, 53, 12026.
- [3] Q. Lin, D. Gourdon, C. Sun, N. Holten-Andersen, T. H. Anderson, J. H. Waite, J. N. Israelachvili, *Proc. Natl. Acad. Sci. USA* **2007**, 104, 3782.
- [4] H. Zeng, D. S. Hwang, J. N. Israelachvili, J. H. Waite, *Proc. Natl. Acad. Sci. USA* **2010**, 107, 12850.
- [5] J. J. Wilker, *Curr. Opin. Chem. Biol.* **2010**, 14, 276.
- [6] J. J. Wilker, *Nat. Chem. Biol.* **2011**, 7, 579.
- [7] J. H. Waite, X.-X. Qin, K. J. Coyne, *Matrix Biol.* **1998**, 17, 93.
- [8] T. Hassenkam, T. Gutschmann, P. Hansma, J. Sagert, J. H. Waite, *Biomacromolecules* **2004**, 5, 1351.
- [9] M. J. Harrington, J. H. Waite, *J. Exp. Biol.* **2007**, 210, 4307.
- [10] E. Vaccaro, J. H. Waite, *Biomacromolecules* **2001**, 2, 906.
- [11] A. Reinecke, L. Bertinetti, P. Fratzl, M. J. Harrington, *J. Struct. Biol.* **2016**, 196, 329.
- [12] M. J. Harrington, H. S. Gupta, P. Fratzl, J. H. Waite, *J. Struct. Biol.* **2009**, 167, 47.
- [13] S. Krauss, T. H. Metzger, P. Fratzl, M. J. Harrington, *Biomacromolecules* **2013**, 14, 1520.
- [14] F. Byette, C. Pellerin, I. Marcotte, *J. Mater. Chem. B* **2014**, 2, 6378.
- [15] F. Byette, A. Laventure, I. Marcotte, C. Pellerin, *Biomacromolecules* **2016**.
- [16] X. Wang, H. J. Kim, C. Wong, C. Vepari, A. Matsumoto, D. L. Kaplan, *Materials Today* **2006**, 9, 44.
- [17] J. F. Almine, D. V. Bax, S. M. Mithieux, L. Nivison-Smith, J. Rnjak, A. Waterhouse, S. G. Wise, A. S. Weiss, *Chem. Soc. Rev.* **2010**, 39, 3371.
- [18] C. Vepari, D. L. Kaplan, *Prog. Polym. Sci.* **2007**, 32, 991.
- [19] C. H. Lee, A. Singla, Y. Lee, *Int. J. Pharm.* **2001**, 221, 1.
- [20] R. Parenteau-Bareil, R. Gauvin, F. Berthod, *Materials* **2010**, 3, 1863.
- [21] G. H. Altman, F. Diaz, C. Jakuba, T. Calabro, R. L. Horan, J. Chen, H. Lu, J. Richmond, D. L. Kaplan, *Biomaterials* **2003**, 24, 401.
- [22] D. N. Woolfson, M. G. Ryadnov, *Curr. Opin. Chem. Biol.* **2006**, 10, 559.
- [23] N. A. Carter, T. Z. Grove, *Biomacromolecules* **2015**, 16, 706.
- [24] S. Lv, D. M. Dudek, Y. Cao, M. M. Balamurali, J. Gosline, H. Li, *Nature* **2010**, 465, 69.
- [25] N. K. Dutta, N. R. Choudhury, M. Y. Truong, M. Kim, C. M. Elvin, A. J. Hill, *Biomaterials* **2009**, 30, 4868.
- [26] T. Z. Grove, L. Regan, A. L. Cortajarena, *J. R. Soc. Interface* **2013**, 10, 20130051.
- [27] T. P. J. Knowles, T. W. Oppenheim, A. K. Buell, D. Y. Chirgadze, M. E. Welland, *Nat. Nanotechnol.* **2010**, 5, 204.
- [28] V. Chiono, E. Pulieri, G. Vozzi, G. Ciardelli, A. Ahluwalia, P. Giusti, *J. Mater. Sci. Mater. Med.* **2008**, 19, 889.
- [29] D. Ding, P. A. Guerette, J. Fu, L. Zhang, S. A. Irvine, A. Miserez, *Adv. Mater.* **2015**, 27, 3953.



- [30] B. P. Partlow, C. W. Hanna, J. Rnjak-Kovacina, J. E. Moreau, M. B. Applegate, K. A. Burke, B. Marelli, A. N. Mitropoulos, F. G. Omenetto, D. L. Kaplan, *Adv. Funct. Mater.* **2014**, *24*, 4615.
- [31] P. Taddei, V. Chiono, A. Anghileri, G. Vozzi, G. Freddi, G. Ciardelli, *Macromol. Biosci.* **2013**, *13*, 1492.
- [32] R. M. Dunn, *Plast. Reconstr. Surg.* **2012**, *130*, 18S.
- [33] S. K. Gorgieva, Vanja In Biomaterials Applications for Nanomedicine; R. Pignatello, Ed.; InTech, 2011, p 17.
- [34] C. N. Grover, J. H. Gwynne, N. Pugh, S. Hamaia, R. W. Farndale, S. M. Best, R. E. Cameron, *Acta Biomater.* **2012**, *8*, 3080.
- [35] J. S. Pieper, T. Hafmans, J. H. Veerkamp, T. H. van Kuppevelt, *Biomaterials* **2000**, *21*, 581.
- [36] J. S. Pieper, P. M. van der Kraan, T. Hafmans, J. Kamp, P. Buma, J. L. C. van Susante, W. B. van den Berg, J. H. Veerkamp, T. H. van Kuppevelt, *Biomaterials* **2002**, *23*, 3183.
- [37] S. Ber, G. Torun Kose, V. Hasirci, *Biomaterials* **2005**, *26*, 1977.
- [38] F. Everaerts, M. Torrianni, M. van Luyn, P. van Wachem, J. Feijen, M. Hendriks, *Biomaterials* **2004**, *25*, 5523.
- [39] Q. Lu, K. Ganesan, D. T. Simionescu, N. R. Vyavahare, *Biomaterials* **2004**, *25*, 5227.
- [40] W. A. Bubnis, C. M. Ofner Iii, *Anal. Biochem.* **1992**, *207*, 129.
- [41] R. Zeeman, P. J. Dijkstra, P. B. van Wachem, M. J. A. van Luyn, M. Hendriks, P. T. Cahalan, J. Feijen, *Biomaterials* **1999**, *20*, 921.
- [42] K. S. Anseth, C. N. Bowman, L. Brannon-Peppas, *Biomaterials* **1996**, *17*, 1647.
- [43] A. A. Arnold, F. Byette, M.-O. Séguin-Heine, A. LeBlanc, L. Sleno, R. Tremblay, C. Pellerin, I. Marcotte, *Biomacromolecules* **2013**, *14*, 132.
- [44] A. Hagenau, P. Papadopoulos, F. Kremer, T. Scheibel, *J. Struct. Biol.* **2011**, *175*, 339.
- [45] M. Jackson, H. H. Mantsch, *Crit. Rev. Biochem. Mol. Biol.* **1995**, *30*, 95.
- [46] H. Fabian, W. Mäntele. In Handbook of Vibrational Spectroscopy; J. M. Chalmers, P. R. Griffiths, Eds.; John Wiley & Sons Ltd: Chichester, 2002, p 27.
- [47] M. A. Bryan, J. W. Brauner, G. Anderle, C. R. Flach, B. Brodsky, R. Mendelsohn, *J. Am. Chem. Soc.* **2007**, *129*, 7877.
- [48] Y. A. Lazarev, B. A. Grishkovsky, T. B. Khromova, *Biopolymers* **1985**, *24*, 1449.
- [49] J. H. Muyonga, C. G. B. Cole, K. G. Duodu, *Food Chem.* **2004**, *86*, 325.
- [50] K. J. Payne, A. Veis, *Biopolymers* **1988**, *27*, 1749.
- [51] S. J. Whittington, B. W. Chellgren, V. M. Hermann, T. P. Creamer, *Biochemistry* **2005**, *44*, 6269.
- [52] L. L. H. D. Olde Damink, P. J.; van Luyn, M. J. A.; van Wachem, P. B.; Nieuwenhuis, P.; Feijen, J., *Biomaterials* **1996**, *17*, 679.
- [53] S.-N. Park, J.-C. Park, H. O. Kim, M. J. Song, H. Suh, *Biomaterials* **2002**, *23*, 1205.
- [54] J. M. Lee, H. H. L. Edwards, C. A. Pereira, S. I. Samii, *J. Mater. Sci. Mater. Med.* **1996**, *7*, 531.